

Cross sections for the ${}^7\text{Li}(p,n){}^7\text{Be}$ reaction between 4.2 and 26 MeV[†]

C. H. Poppe,* J. D. Anderson, J. C. Davis, S. M. Grimes, and C. Wong
Lawrence Livermore Laboratory, Livermore, California 94550
 (Received 26 April 1976)

Using pulsed-beam neutron time-of-flight spectrometry relative differential cross sections for ${}^7\text{Li}(p, n_0){}^7\text{Be}(\text{g.s.})$ and ${}^7\text{Li}(p, n_1){}^7\text{Be}^*$ (0.431 MeV) have been measured over the laboratory angular range 3.5° to 159° and from an incident bombarding energy of 4.2 to 26 MeV. These cross sections have been integrated over angle and at 5 MeV the resulting integral was normalized to the absolute measurement of Macklin and Gibbons in order to obtain absolute differential and total cross sections for each neutron group. At energies above 6 MeV the 3.5° cross section for each group decreases monotonically, reaching a minimum at about 12 MeV. Both cross sections then increase, the ground-state cross section approaching a center-of-mass value of 15 mb/sr at 26 MeV. The forward-angle ratio of n_1 to n_0 neutrons remains around 30% from 8 to 26 MeV, obtaining a maximum of about 35% at 26 MeV. The integrated cross sections, on the other hand, both decrease from 6 MeV to the maximum energy. Neutrons from states in ${}^7\text{Be}$ at 4.55, 6.51, 7.19, and possibly 10.79 MeV as well as those from three-body breakup were also observed in this experiment.

[NUCLEAR REACTIONS ${}^7\text{Li}(p, n)E = 4.2\text{--}26$ MeV; measured $\sigma(E, \theta)$ to ${}^7\text{Be}$ ground state and first excited state; $\theta = 3.5^\circ\text{--}159^\circ$.]

I. INTRODUCTION

At low energies the ${}^7\text{Li}(p, n){}^7\text{Be}$ reaction has long been used as a source of neutrons.¹ Between 1.9- and 2.4-MeV bombarding energy the neutrons are monoenergetic and the reaction has a large cross section. Above 2.4 MeV the first-excited state of ${}^7\text{Be}$ at 0.43 MeV may be excited, producing a second group of neutrons; however, below 5 MeV the 0° yield of these lower energy neutrons is less than about 10% of the ground-state yield, so that the usefulness of the reaction as a monoenergetic neutron source is only slightly impaired. The many experiments at low energy have been summarized in a recent article by Burke, Lunnon, and Lefevre,² and a large body of data between threshold (1.881 MeV) and 7 MeV have been evaluated by Liskien and Paulsen.³

Above 6 MeV, there are few measurements on this reaction. Bair, Jones, and Willard⁴ measured the total neutron yield from proton bombardment of ${}^7\text{Li}$ between 4 and 14 MeV, but this measurement includes neutrons from excitation of higher excited states of ${}^7\text{Be}$ as well as those produced in three-body breakup reactions. Borchers and Poppe⁵ used time-of-flight techniques to separate the ground-state neutrons (n_0) from the neutrons which leave ${}^7\text{Be}$ in the first excited state (n_1) and measured relative differential cross sections for each group between 4 and 10 MeV. These data were normalized to the absolute measurements of Macklin and Gibbons⁶ between 4.5 and 5 MeV.

Time-of-flight measurements at Livermore⁷ in 1965 extend the differential cross section of the two neutron groups to 14 MeV and recent measurements at Tashkent⁸ have been reported at 14.9 and 17.8 MeV. At higher energies the neutron groups have not been resolved in measurements reported to date.⁹⁻¹³ Such a separation is necessary in order to study the utility of the ${}^7\text{Li}(p, n){}^7\text{Be}$ reaction as a neutron source at higher energies. In this paper we report the measurement of relative differential cross sections for the two groups n_0 and n_1 , at energies between 4.25 and 26 MeV.

II. EXPERIMENTAL METHOD

Between 4.25 and 12 MeV protons were accelerated using an EN tandem Van de Graaff accelerator. In order to reach the higher energies the tandem injector is replaced by a 15-MeV AVF cyclotron and the cyclograaff then produced protons of energies between 15.2 and 26 MeV. Consequently, there is a 3-MeV gap in the data between the highest tandem energy and the lowest cyclograaff energy. Neutron energy spectra at 16 angles between 3.5° and 159° were obtained simultaneously by measuring the time of flight over the 10.8-m flight path between target and each of 16 detectors. The beam pulsing systems for accelerator configurations and the time-of-flight capabilities are described in a paper by Davis *et al.*¹⁴ NE213 scintillators were used as detectors and pulse-shape

discrimination was used to reduce background from pulses produced by γ rays.

The targets were self-supporting metallic foils of 99.87% ${}^7\text{Li}$, approximately 2.3 mg/cm^2 for the tandem runs and 4.7 mg/cm^2 for the cyclograaff runs. Because of rapid deterioration of the targets after the experiment no absolute determination of the target thickness was made. The areal densities just quoted were inferred after the relative measurements were normalized to Gibbons and Macklin. To verify that target deterioration did not occur during the measurements, comparison spectra from an LiF target were also taken at many of the bombarding energies, and a final run with the Li targets was taken at the energy at which the first measurements were made.

A Faraday cup about 3 m from the target stopped the proton beam. Because the neutron detectors are located behind 2-m long water-filled collimators in a thick concrete shield wall, neutrons produced at the Faraday cup are greatly attenuated before reaching the detectors. The collimation and massive shielding also reduce the background caused by room scattered neutrons. Consequently, neutron background in the portion of the spectrum corresponding to the n_0 and n_1 groups was very small, typically less than 1% of the sum of the n_0 and n_1 counts, and if present at all was subtracted by a linear interpolation of the counts per channel in the channels on either side of the peaks of interest.

Figure 1 shows a typical neutron energy spectrum obtained in a tandem run—no background has been subtracted. The energy calibration has been determined by a time calibration based on the target γ ray peak (not shown) and that of the following beam burst (not shown). Variation of detector efficiency with neutron energy, inferred target thickness, and conversion from time of flight to energy have been included to convert the ordinate to units of $\text{mb sr}^{-1}\text{ MeV}^{-1}$. Points shown are averages of the data over 100-keV intervals. For this run the neutron detector bias was at a neutron energy of 2.5 MeV. At this energy the n_0 and n_1 groups are easily resolved and the background is negligible. Also present in the spectrum are neutrons from the second-excited state of ${}^7\text{Be}$ at 4.55 MeV and continuum neutrons from breakup reactions. Arrows in the figure indicate the calculated energies of neutrons from the ${}^7\text{Be}$ excited states as well as the maximum possible energy of neutrons from the ${}^7\text{Li}(p,n\alpha){}^3\text{He}$ three-body reaction.

Because the n_0 and n_1 neutron groups were not completely resolved for the cyclograaff runs it was necessary to use a peak fitting program to obtain cross sections for these groups at forward

angles. Parameters used in the fit included the slope and height of a linear background and the height and location of each of the two peaks and a common width for both. It was assumed that in a time-of-flight spectrum each peak has a Gaussian shape, based on the fact that the observed peak widths were caused primarily by time width of the beam pulses, with a smaller contribution from target thickness effects. Under these circumstances the contribution from the intrinsic width of the levels was negligible. In addition, peak shapes in the back angle detectors, in which the peaks were well resolved because of the lower neutron energies, were essentially Gaussian.

Typical fitting intervals were about 35 channels. Over this region it was usually possible to obtain reduced χ^2 values of between 1 and 2.5 using a search procedure based on the technique proposed by Marquart as described by Bevington.¹⁵ Fits

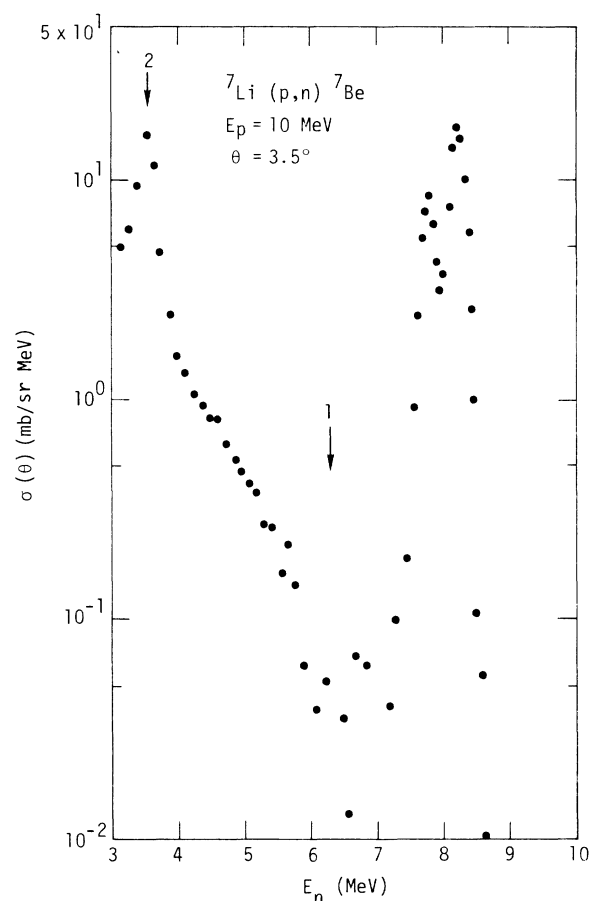


FIG. 1. Laboratory neutron spectrum from the ${}^7\text{Li}(p,n){}^7\text{Be}$ reaction at 3.5° for 10-MeV protons. The arrow labeled 1 denotes the calculated endpoint for the ${}^7\text{Li}(p,n+{}^3\text{He}+{}^4\text{He})$ reaction and that denoted 2 indicates the neutron group for reactions populating the 4.55-MeV state in ${}^7\text{Be}$.

were subject to the constraint that the two peaks have a fixed separation (determined by the known energy difference between the levels). These results agreed within errors with those from unconstrained fits. In another check, the fits were repeated with the addition of a tail to the Gaussian peaks. A significant reduction in χ^2 values was achieved for tails with about 3 to 5% of the peak area; however, inclusion of the tail did not affect significantly the absolute contributions of n_0 and n_1 extracted from the fits, so the values obtained from the fits without tails were used in calculating cross sections.

The peak separation procedure was checked by taking data at the same energies using a 29-m flight path at 0° . For this flight path, the n_0 and n_1 groups could easily be resolved and the resulting n_0 to n_1 ratio compared to the results of the Gaussian peak fitting procedure. In order to compare the two sets of ratios, the total χ^2 was calculated using the differences between the long-flight-path ratio and the Gaussian peak ratio, weighted by the statistical error in the long-flight-path ratio. The resulting value of χ^2 per point for the eleven measurements was 1.20, demonstrating agreement of the two methods within the statistical errors of the long-flight-path measurements. It is difficult to estimate the errors introduced in the peak-fitting routine, especially at the highest cyclograaff energies, but an upper

limit is felt to be about 10% for n_0 and 20% for n_1 .

Figure 2 shows a typical neutron energy spectrum obtained in a cyclograaff run. The smooth curves illustrate the results of the peak-fitting procedure described in the preceding paragraphs. In addition to arrows indicating the same excited states and breakup reactions as Fig. 1, the calculated energies of the third and fourth excited states in ${}^7\text{Be}$ at 6.51 and 7.19 MeV, respectively, and the endpoint of the ${}^7\text{Li}(p, pn) {}^6\text{Li}$ reaction are similarly indicated. There is also evidence for the excitation of the first $T = \frac{3}{2}$ state of ${}^7\text{Be}$. This state occurs at an excitation energy of 10.79 MeV and is the isobaric analog of the ${}^7\text{He}$ and ${}^7\text{B}$ ground states. Its predicted energy is indicated in the figure by the arrow near 8.7-MeV neutron energy.

Relative differential cross sections were calculated from the counts in the peaks using the previously determined detector efficiencies¹⁶ and nominal target thickness. The angular distributions obtained at 5 MeV for the n_0 and n_1 groups were integrated over angle and then summed together to obtain a relative total neutron production cross section. This number was then compared to the absolute measurement of Macklin and Gibbons⁶ to obtain a normalization factor for the target used on the tandem runs.¹⁷ At 16 MeV, runs on the cyclograaff were taken with both targets so that the thicker target could also be normalized to the 5-MeV point. As a check, both targets were again

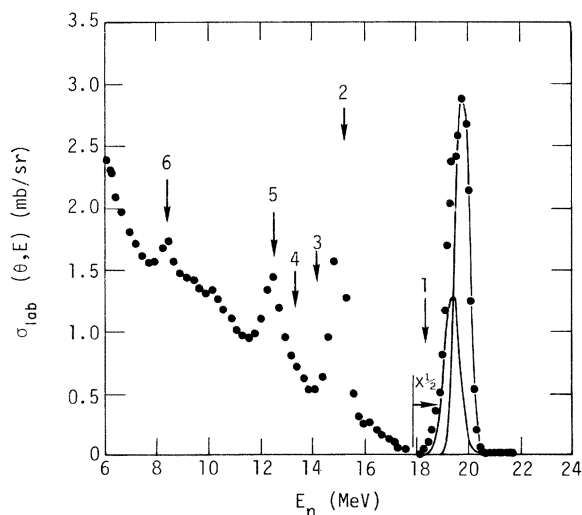


FIG. 2. Same as Fig. 1, except that the proton energy is 22 MeV and the angle 23° . The arrows numbered 1 through 6 denote, respectively, neutron energies corresponding to the endpoint of the ${}^7\text{Li}(p, n + {}^3\text{He} + {}^4\text{He})$ reaction spectrum, the population of the 4.55-MeV state in ${}^7\text{Be}$, the endpoint of the ${}^7\text{Li}(p, n + p + {}^6\text{Li})$ reaction spectrum, and population of the 6.51, 7.19, and 10.79 states in ${}^7\text{Be}$. The latter state is the lowest $T = \frac{3}{2}$ state in ${}^7\text{Be}$.

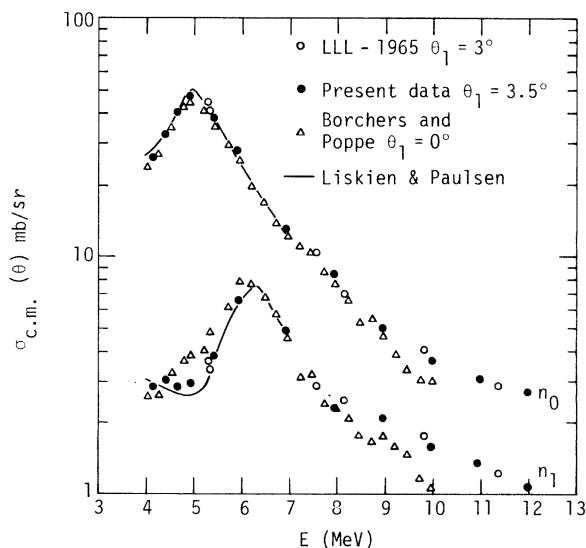


FIG. 3. Excitation functions for the ${}^7\text{Li}(p, n_0)$ and ${}^7\text{Li}(p, n_1)$ reaction between 4 and 12 MeV. The solid line represents the recommended values of Liskien and Paulsen and the open circles, closed circles, and \times marks denote the measurements of Anderson *et al.*, the present data, and Borchers and Poppe, respectively.

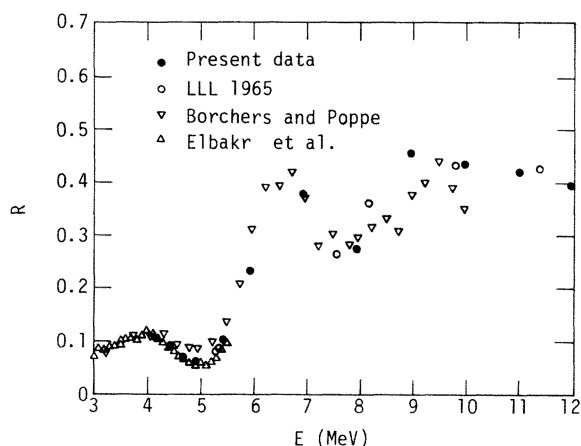


FIG. 4. The ratio of the cross section for the ${}^7\text{Li}(p,n)$ reaction to the first-excited state of ${}^7\text{Be}$ to that of the ground state between 3 and 12 MeV. The data include those of Refs. 5, 7, and 18 in addition to the present measurements.

measured at 9 MeV on the tandem and a thick-thin target ratio within 4% of that determined at 16 MeV was found.

Major sources of error in the tandem runs are errors in integrating the 5-MeV angular distribution and normalizing to the Macklin and Gibbons measurement, counting statistics, and uncertainty in the variation of detector efficiency from detector to detector and with neutron energy. Background and peak separation errors are relatively

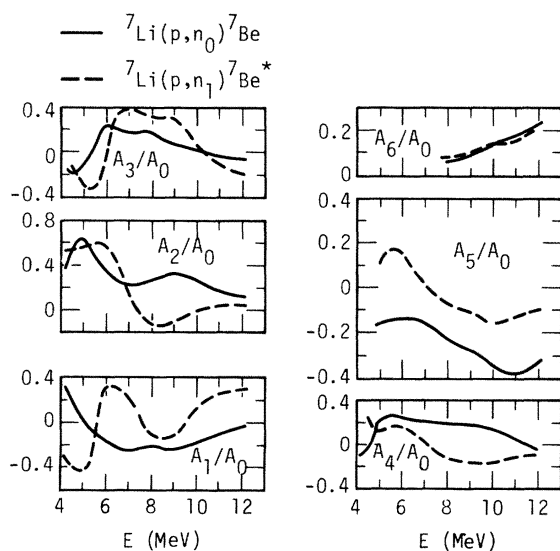


FIG. 5. Coefficients of Legendre expansions in the center-of-mass system of the present data between 4 and 12 MeV. The solid line denotes the ground-state group, while the dashed line represents the expansion for the first-excited state group.

minor. Total errors in the tandem relative cross sections are estimated to be about 4%. For the cyclograaff runs, peak separation becomes the major source of error and uncertainties in the normalization of the thick to thin target of somewhat less importance. An average error of about 8% is estimated for the cyclograaff runs, but it is felt that errors at the lower cyclograaff energies are somewhat better than this, whereas those for the n_1 group at the higher energies are probably worse.

As a check on the absolute magnitude of the cross sections reported here (determined by normalization of the 5-MeV data) the cross sections obtained from the LiF target (which had been weighed to determine the target thickness to 5% accuracy) were compared to those from the Li targets. At forward angles, the ${}^7\text{Li}(p,n_0)$ and ${}^7\text{Li}(p,n_1)$ groups are separated from ${}^{19}\text{F}(p,n)$ neutron groups. The average ratio of the 3.5° cross sections presented in this paper to the LiF absolute measurements was found to be 1.02, well within the errors.

III. RESULTS

A. Tandem data

Figure 3 shows the normalized center-of-mass differential cross sections for the ground-state and first-excited state neutron groups obtained on the tandem at a laboratory reaction angle of 3.5° . Also shown are the corresponding 0° data of Borchers and Poppe.⁵ Although agreement in shape is good

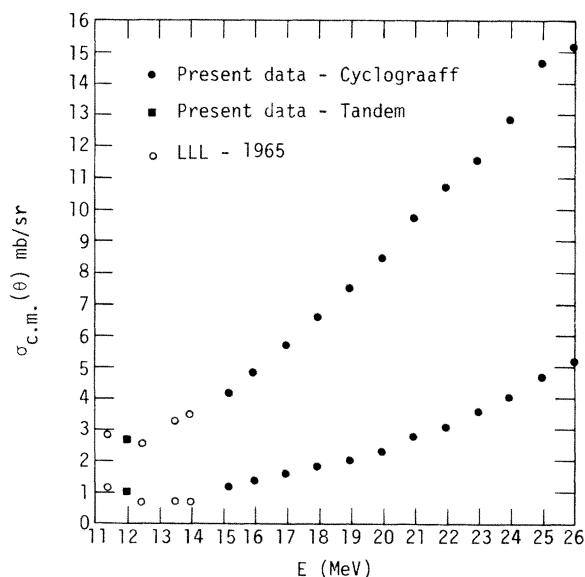


FIG. 6. Cross sections at 3.5° for the ${}^7\text{Li}(p,n_0)$ and ${}^7\text{Li}(p,n_1)$ reactions between 11 and 26 MeV.

for the ground-state group between 4.25 and about 8 MeV, the present measurements are somewhat larger in magnitude. This may seem puzzling in view of the identical normalization of the two data sets, but is explained by the fact the present data yield an angular distribution somewhat more forward peaked than the former and, in addition, the data of Ref. 5 report a substantially larger cross section for the n_1 group in the region of normalization of n_0 to the total cross section. Agreement of the present data with the recommended cross

section (solid curves) of Liskien and Paulsen³ is excellent for both the n_0 and n_1 groups.

Above 8 MeV the data of Ref. 5 consistently fall below the present measurements for both neutron groups. Figure 3 also illustrates the previous Livermore relative measurements⁷ at 3° which were normalized in magnitude to the present data and although obtained on another accelerator with different detectors agree in shape with the present measurements over the entire tandem energy range.

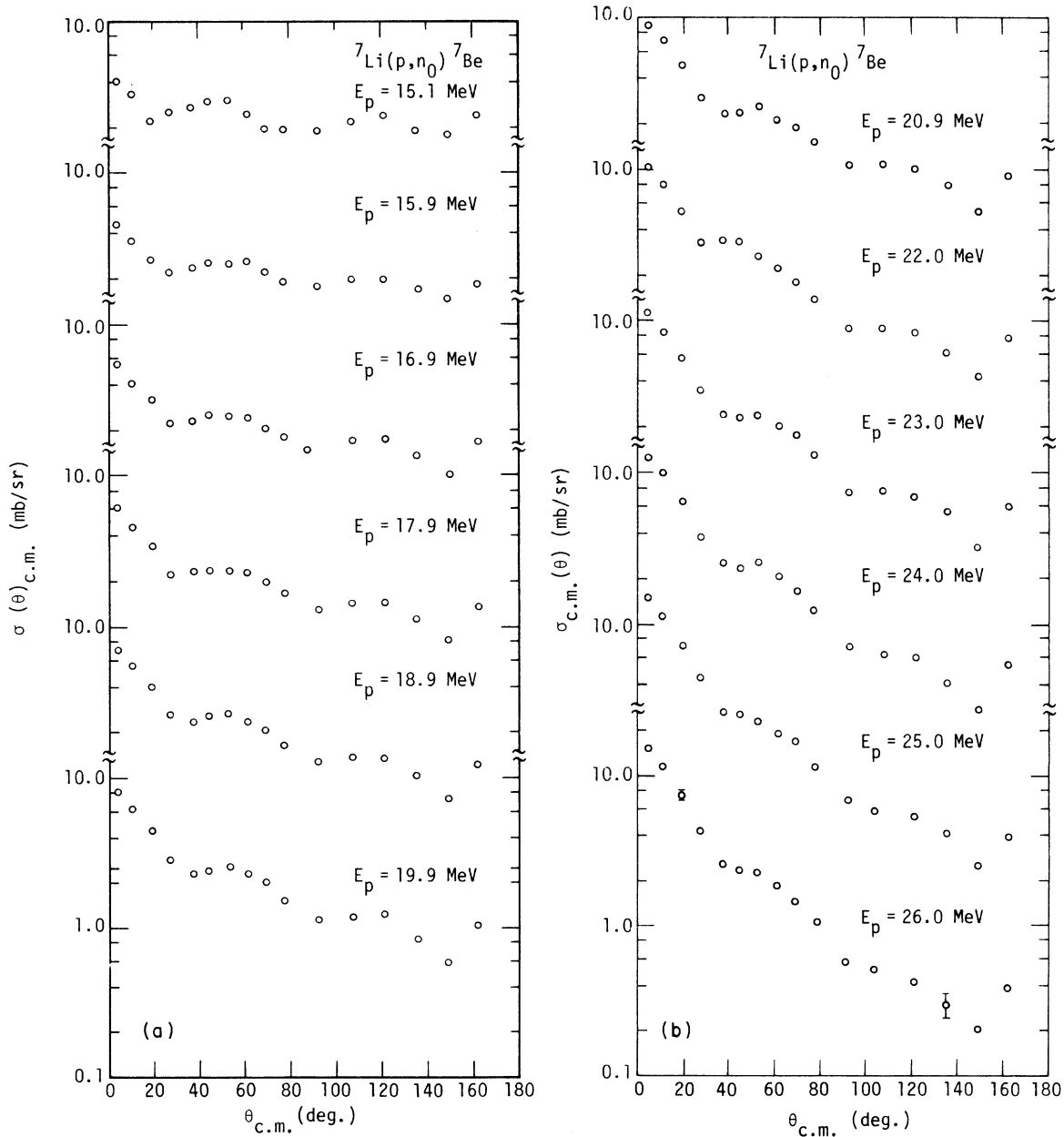


FIG. 7. Center-of-mass angular distributions for the ${}^7\text{Li}(p, n_0){}^7\text{Be}$ reaction between 15 and 26 MeV. (a) Cross sections for proton energies between 15 and 20 MeV. (b) Cross sections for proton energies between 21 and 26 MeV.

Figure 4 presents the ratio of the n_1 to n_0 center-of-mass cross sections, the ratio being independent of any normalization or target thickness problems and approximately independent of the neutron detector efficiency. In addition to the data of Fig. 3, there are plotted in Fig. 4 the results of Elbahr *et al.*¹⁸ at 0° . At energies between 4.5 and 5.5 MeV, where peak separation should be no problem and errors are small, the present data

and those of Refs. 17 and 7 all agree very well, but fall below the ratios of Ref. 5 which appear to remain high out to 7 MeV. Between 7 and 12 MeV there is considerable scatter and agreement is fair between different sets of data, but the errors due to peak separation are becoming fairly large in the data of Ref. 5 because of poorer resolution.

The center-of-mass angular distributions of both the n_0 and n_1 groups were fitted by a series of

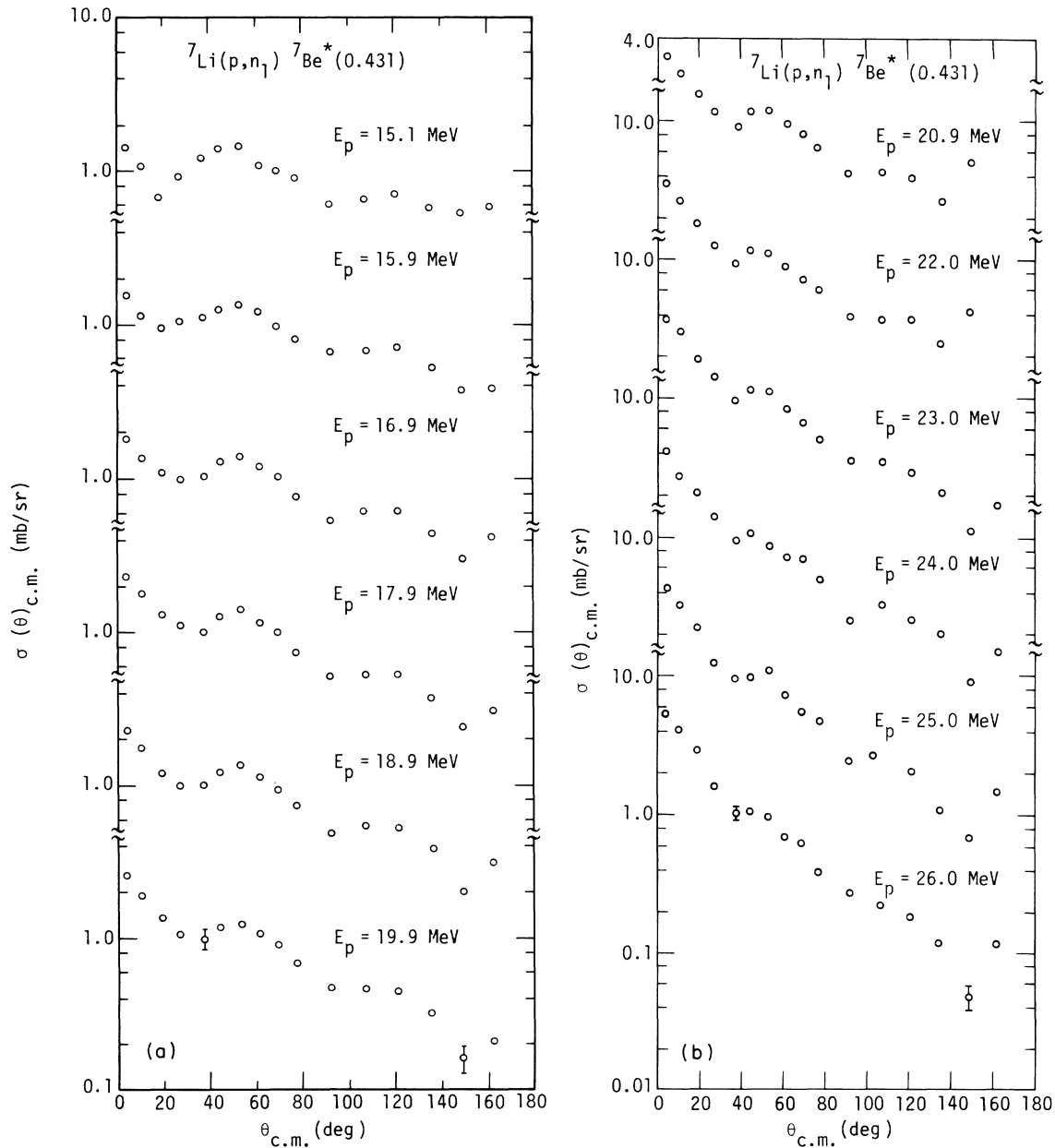


FIG. 8. Same as Fig. 7 for the ${}^7\text{Li}(p,n){}^7\text{Be}$ reaction. (a) Cross sections for proton energies between 15 and 20 MeV. (b) Cross sections for proton energies between 21 and 26 MeV.

Legendre polynomials,

$$\sigma_{c.m.} = \sum_{n=0}^N A_n P_n(\cos\theta).$$

It follows that $\sigma_T = 4\pi A_0$, where σ_T is the integrated cross section. For energies below about 4.75 MeV, the angular distributions required polynomials up to $N=4$; between 5 and 7 MeV, $N=5$ was needed; and between 8 and 12 MeV, $N=6$ gradually became important. The ratios A_n/A_0 are plotted as a function of bombarding energy in Fig. 5.

B. Cyclograaff data

Figure 6 shows the $3.5^\circ(\text{lab})$ n_0 and n_1 center-of-mass cross sections as a function of bombarding energy for the higher energy data taken on the cyclograaff. In order to bridge the gap between the tandem and cyclograaff results, the n_0 data of Ref. 7 at 3° were normalized between 5 and 11 MeV to the present tandem data (see Fig. 3) and are also plotted in Fig. 6. One sees that after a minimum at about 12 MeV, the forward n_0 cross section rises again approaching 15 mb/sr. However, although fluctuating, the n_1 to n_0 ratio remains substantial at about 30%.

As in the case of the tandem data, the angular distributions were fitted with a Legendre polynomial series in order to determine the integrated cross sections. However, the usefulness of this as a means of presenting data is limited at the higher energies as more and more polynomials are required to reproduce the data. Center-of-mass angular distributions are plotted for the cyclograaff runs for the n_0 group in Fig. 7 and for the n_1 group in Fig.

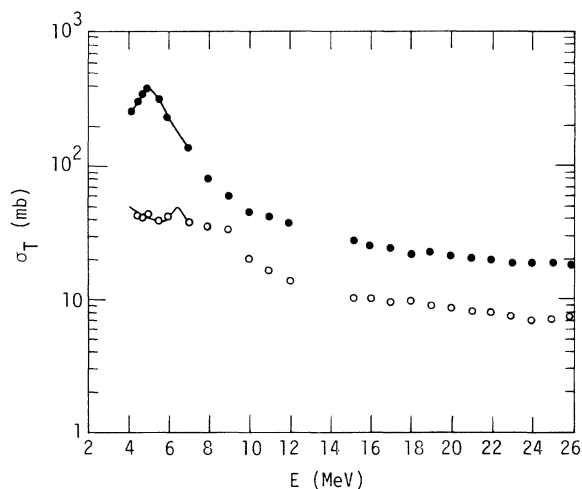


FIG. 9. Total cross sections for the ${}^7\text{Li}(p, n_0){}^7\text{Be}$ and ${}^7\text{Li}(p, n_1){}^7\text{Be}$ reactions between 4 and 26 MeV. The solid lines represent the recommendations of Liskien and Paulsen.

TABLE I. Laboratory differential cross section at 3.5° for the ${}^7\text{Li}(p, n){}^7\text{Be}$ (0.0 MeV + 0.43 MeV) reaction and the laboratory ratio of n_1 to n_0 neutrons as a function of bombarding energy.

E_p (MeV)	$\sigma_0 + \sigma_1$ (mb/sr)	R
15.1	7.38	0.30
15.9	8.2	0.28
16.9	9.7	0.26
17.9	11.1	0.27
18.9	12.6	0.27
19.9	14.3	0.27
20.9	15.9	0.27
21.9	18.2	0.29
22.9	20.1	0.30
23.9	22.4	0.30
24.9	25.5	0.32
25.9	26.9	0.35

8. One sees that at each energy the angular distribution of the n_1 group is quite similar to that of the n_0 group in distinct contrast to the lower energy data. A trend towards isotropy as the energy increases from 6 to 10 MeV was pointed out by Borchers and Poppe⁵; however, as the energy increases further a strong forward peaking appears and the diffractionlike structure becomes prominent.

C. Integrated cross sections

From the Legendre polynomial fits of both the tandem and cyclograaff angular distributions the integrated cross section for each neutron group was extracted at each energy. These results are presented in Fig. 9, where, in contrast to the 3.5° differential cross section, the integrated cross section for each group decreases monotonically above 5 MeV. The 3.5° cross section behavior simply reflects the onset of the strong forward peaking. Above 7 MeV, the total number of neutrons which leave ${}^7\text{Be}$ in the first-excited state is always greater than 25% of the number of neutrons which leave ${}^7\text{Be}$ in the ground state, reaching a maximum of 55% at 9 MeV. Also shown as the solid curve in Fig. 9 are the recommended integrated cross sections of Liskien and Paulsen.³

IV. CONCLUSION

The usefulness of the ${}^7\text{Li}(p, n){}^7\text{Be}$ reaction as a neutron source at high energies would depend on the particular application. Only very good energy resolution would allow one to separate the substantial number of n_1 neutrons to obtain a monoenergetic source. However, if the application can tolerate including both neutron groups, then the reaction has the favorable features of use of a

solid target with a forward angle laboratory cross section approaching 30 mb/sr. Table I presents the 3.5° laboratory differential cross section for the sum of both neutron groups and the laboratory n_1 to n_0 ratio for the cyclograaff energies. These data would extrapolate to about 30 mb/sr at 29 MeV which is about 30% less than that reported by Jungerman *et al.*¹² using a proton-recoil telescope. Other measurements^{10, 11, 13} near 29 MeV agree within errors with the extrapolated value of the

present measurements. The measurements of ${}^7\text{Li}(p, n_1)$ at 23 and 25 MeV of Locard, Austin, and Benenson¹⁹ are also in agreement with the present data. Although the cross section is large, the presence of lower energy neutrons, the contribution of which is indicated in Fig. 2, may limit the usefulness of the ${}^7\text{Li}(p, n){}^7\text{Be}$ reaction as a monoenergetic neutron source at energies between 10 and 30 MeV.

*On sabbatical leave from University of Minnesota.

†Work performed under the auspices of the U. S. Energy Research and Development Administration under contract W-7405-ENG-48.

¹J. H. Gibbons and H. W. Newson, *Fast Neutron Physics I*, edited by J. B. Marion and J. L. Fowler (Interscience, New York, 1960), p. 133.

²C. A. Burke, M. T. Lunnion, and H. W. Lefevre, *Phys. Rev. C* **10**, 1299 (1974).

³H. Liskien and A. Paulsen, *At. Data Nucl. Data Tables* **15**, 57 (1975). A preliminary account of this evaluation appeared as EANDC Report No. 159“L”. There are some minor differences between the above publication and the preliminary report.

⁴J. K. Bair, C. M. Jones, and H. B. Willard, *Nucl. Phys.* **53**, 209 (1964).

⁵R. R. Borchers and C. H. Poppe, *Phys. Rev.* **129**, 2679 (1963).

⁶J. H. Gibbons and R. L. Macklin, *Phys. Rev.* **114**, 571 (1959).

⁷J. D. Anderson, C. Wong, and V. A. Madsen, *Phys. Rev. Lett.* **24**, 1074 (1970). Only a portion of data referred to here appear in this publication. The remaining data were unpublished.

⁸U. R. Arifkhanov, M. Gulyamov, B. I. Islamov, M. Kayumov, and E. Ertashov, *Yad. Fiz.* **19**, 25 (1974) [*Sov. J. Nucl. Phys.* **19**, 12 (1974)].

⁹J. W. Wachter, R. T. Santoro, T. A. Love, and W. Zobel, *Nucl. Instrum. Methods* **113**, 185 (1973).

¹⁰C. J. Batty, B. E. Bonner, E. Friedman, C. Tschalär,

L. E. Williams, A. S. Clough, and J. B. Hunt, *Nucl. Phys.* **A120**, 297 (1968).

¹¹C. J. Batty, B. E. Bonner, A. I. Kilvington, C. Tschalär; and L. E. Williams, *Nucl. Instrum. Methods* **68**, 273 (1969).

¹²J. A. Jungerman, F. P. Brady, W. J. Knox, T. Montgomery, M. R. McGie, J. L. Romero, and Y. Ishizaki, *Nucl. Instrum. Methods* **94**, 421 (1971).

¹³M. W. McNaughton, N. S. P. King, F. P. Brady, J. C. Romero, and T. S. Subramanian, *Nucl. Instrum. Methods* **130**, 555 (1976).

¹⁴J. C. Davis, J. D. Anderson, E. K. Freytag, and D. R. Rawles, *IEEE Trans. Nucl. Sci.* **20**, 213 (1973).

¹⁵P. R. Bevington, *Data Reduction and Error Analysis for the Physical Sciences* (McGraw-Hill, New York, 1969), p. 235.

¹⁶C. Wong, J. D. Anderson, J. C. Davis, and S. M. Grimes, *Phys. Rev. C* **7**, 1895 (1973).

¹⁷A redetermination of the efficiency of the neutron detector used in Ref. 6 and reported in Ref. 2 would increase the magnitude of cross sections of the present measurements by 2%. This change has not been made in the paper because the errors are greater than the increase.

¹⁸S. A. Elbakr, I. J. Van Heerden, W. J. MacDonald, and G. C. Neilson, *Nucl. Instrum. Methods* **105**, 519 (1972).

¹⁹P. J. Locard, S. M. Austin, and W. Benenson, *Phys. Rev. Lett.* **19**, 1141 (1967).